III. Conclusion

This communication presented a microstrip-fed millimeter-wave Yagi-Uda antenna with applications as single element radiator or for switched-beam systems with medium gain (9–13 dB). The planar Yagi-Uda antenna can be arrayed for additional gain (+3 dB) and with low mutual coupling between the elements. The antenna results in relatively wideband operation (22–26 GHz), low cross-polarization levels, and high radiation efficiency. This antenna can be scaled to 60, 77, or 94 GHz for automotive radars and high data-rate communication systems.

References

[1] N. Kaneda, W. R. Deal, Y. Qian, R. Waterhouse, and T. Itoh, "A broadband planar Quasi-Yagi antenna," *IEEE Trans. Antennas Propag.*, vol. 50, no. 8, pp. 1158–1160, Aug. 2002.

[2] P. R. Grajek, B. Schoenlinner, and G. M. Rebeiz, "A 24-GHz high-gain Yagi-Uda antenna array," *IEEE Trans. Antennas Propag.*, vol. 52, pp. 1257–1261, May 2004.

[3] G. Zheng, A. A. Kishk, A. B. Yakovlev, and A. W. Glisson, "Simplified feed for a modified printed Yagi antenna," *Electron. Lett.*, vol. 40, no. 8, pp. 464–465, Apr. 15, 2004.

[4] Y. Lee and S. Chung, "Design of a 38-GHz printed Yagi antenna with multiple directors," in *Proc. IEEE Antennas Propag. Symp.*, Jul. 2001, vol. 3, pp. 606–609.

[5] G. R. DeJean and M. M. Tentzeris, "A new high-gain microstrip Yagi array antenna with a high front-to-back (F/B) ratio for WLAN and millimeter-wave applications," *IEEE Trans. Antennas Propag.*, vol. 55, pp. 298–304, Feb. 2007.

[6] D. Woo, Y. Kim, K. Kim, and Y. Cho, "A simplified design of Quasi-Yagi antennas using the new microstrip-to-CPS transitions," in *Proc. IEEE Antennas Propag. Symp.*, June 2007, pp. 781–784.

[7] H. K. Kan, R. B. Waterhouse, A. M. Abbosh, and M. E. Bialkowski, "Simple broadband planar CPW-fed Quasi-Yagi antenna," *IEEE Antennas Wireless Propag. Lett.*, vol. 6, pp. 18–20, 2007.

[8] S. Hsu, K. Wei, C. Hsu, and R. Chuang, "A 60-GHz millimeter-wave CPW-Fed Yagi antenna fabricated by using 0.18-μm CMOS technology," *IEEE Electron. Device Lett.*, vol. 29, pp. 625–627, Jun. 2008.

[9] W. L. Stutzman and G. A. Thiele, *Antenna Theory and Design*, 2nd ed. New York: Wiley, 1998.

On the Transmission and Propagation of Low Attenuation Rate Electromagnetic Pulses in Debye Media

Reza Safian, Costas D. Sarris, and Mohammad Mojahedi

***Abstract*—In a dispersive medium, the appearance of the steady-state part of the signal is preceded by oscillations known as precursors. These early oscillations are the product of the interrelated effects of phase dispersion and frequency dependent attenuation. Inside water, the attenuation rate of the Brillouin precursor is sub-exponential, following the inverse square-root of the distance traveled. Based on that, a near-optimal pulse that could achieve this attenuation rate, and, hence, would lend itself to underwater detection and communication applications, was recently proposed. The "optimality" of this pulse is shown to be related to the temporal support of the pulse and its spectral characteristics, rather than its shape. A family of alternative pulses is found to have the low attenuation feature of the "optimal" pulse, as they eventually evolve into the Brillouin precursor itself shortly after they enter water. In addition, this work considers the practical case when such a pulse would be generated in air, would impinge onto an air-water interface and then propagate inside water. It is shown how the presence of the interface affects the attenuation rate of the pulse inside water and a simple way to recover its low attenuation rate is suggested. The finite-difference time-domain technique is employed in all the simulations.**

***Index Terms*—Dispersive media, finite-difference time-domain (FDTD) methods, wave propagation.**

I. Introduction

The propagation of wideband electromagnetic pulses in a causal, temporally dispersive dielectric has been studied extensively [1], [2]. Significant contributions in this area have been recently made by Oughstun *et al.*, through the investigation of pulse propagation in several temporally dispersive media [3]. In such media, the phase dispersion and frequency-dependent attenuation of a wideband pulse excitation can lead to the evolution of precursor fields, which precede the main part of the pulse.

For a Debye-type dielectric, the electric field excited by a modulated pulse with a temporal support T where, $T \gg 1/f_c$ (f_c is the modulation frequency) evolves into the so-called Brillouin precursor, as the pulse propagates inside the medium [3]. Moreover, the peak amplitude of the Brillouin precursor decays as the inverse square root of the propagation distance, as opposed to the exponential decay of the main part of the pulse.

This property of the Brillouin precursor was harnessed to design a pulse excitation with low attenuation rate in an infinite Debye medium [4]. Such an excitation consists of two mutually delayed and opposite in sign Brillouin precursors. The theoretical investigation of [4], limited to the case of an infinite Debye medium though, suggested that this "double Brillouin" pulse could indeed achieve an attenuation rate as the inverse square of the propagation distance for medium parameters that corresponded to those of the triply distilled water. This result renders the double Brillouin pulse a good candidate for applications ranging from communications to detection in lossy dispersive media that can be described by the Debye model.

Manuscript received July 09, 2007; revised November 18, 2008. First published July 28, 2009; current version published November 04, 2009.

The authors are with the Department of Electrical and Computer Engineering, University of Toronto, Toronto, ON M5S 3G4 Canada (e-mail: rsafian@waves.utoronto.ca).

Color versions of one or more of the figures in this communication are available online at http://ieeexplore.ieee.org.

Digital Object Identifier 10.1109/TAP.2009.2028678

This communication extends the study of the double Brillouin pulse presented in [4], to investigate the origin of its low attenuation property, and its interaction with an interface between air and a dispersive medium at oblique incidence. First, it is shown that the critical element that provides for the "optimality" of the double Brillouin pulse, in terms of its attenuation rate of the peak of the pulse, is not its shape but its temporal support. Even a simple trapezoidal pulse, with appropriately chosen temporal support, can have similar properties, as it itself eventually evolves into a Brillouin pulse. Second, the differences between the propagation characteristics of the double Brillouin pulse in an infinite medium, compared to its oblique incidence at an air-dispersive medium interface through the finite-difference time-domain (FDTD) method. It is shown that the attenuation rate of the transmitted pulse actually depends on the angle of incidence, deteriorating with respect to the infinite case even at normal incidence. A careful study of this effect leads to its explanation and remedy, through a proposed medium-dependent modification of the shape of the double Brillouin pulse.

II. Effects of the Shape of the Excitation on Attenuation Properties of the Double Brillouin Pulse

For a Rocard–Powles–Debye model dielectric, the complex index of refraction is given by [4]

$$n(\omega) = \left[\epsilon_\infty + \frac{(\epsilon_s - \epsilon_\infty)}{(1 - i\omega\tau)(1 - i\omega\tau_f)}\right]^{1/2} \tag{1}$$

where the $\exp(-i\omega t)$ time convention is used. The index of refraction described by (1) with parameters $\epsilon_\infty = 2.1$, $\epsilon_s = 76.2$, $\tau = 8.44 \times 10^{-12} s$, $\tau_f = 4.62 \times 10^{-14} s$ models triply-distilled water at 25°C [4].

Having specified the dispersion, the next step is to define the excitation which is another parameter that affects the evolution of precursors. The closed form of the double Brillouin pulse, $f_{DB}(t)$, is given in [4]

$$f_{DB}(t) = f_{SB}(t) - f_{SB}(t - T) \tag{2}$$

where $f_{SB}(t)$ is the Brillouin precursor in the medium with dispersion defined in (1) at $z = z_d$. The absorption depth, z_d, is defined based on the attenuation factor at a frequency f_c as

$$z_d = \frac{1}{\alpha(f_c)}. \tag{3}$$

It is approximately 21 cm at 1 GHz with the mentioned medium parameters. The complex wave number is given by

$$\tilde{k}(\omega) = \beta(\omega) + i\alpha(\omega) = \frac{\omega}{c} n(\omega) \tag{4}$$

where $\beta(\omega) = \Re\{\tilde{k}(\omega)\}$ is the plane wave phase constant and $\alpha(\omega) = \Im\{\tilde{k}(\omega)\}$ denotes the attenuation factor. The parameter $T = 1/f_c$ describes the fixed time delay between the leading and trailing-edge single Brillouin pulses.

The effect of the time delay between the two single Brillouin pulses on the attenuation rate of the double Brillouin pulse is discussed in [4]. A relevant question is whether alternative (and potentially simpler) excitation forms could produce a pulse with an attenuation rate similar to that of the near optimal pulse of [4] inside water.

To address this question, the propagation of a "double trapezoidal" pulse inside water is studied. This pulse consists of two "single trapezoidal" pulses, that are mutually delayed by $T = 1/f_c$ and opposite in sign. Mathematically, the single trapezoidal pulse is defined as

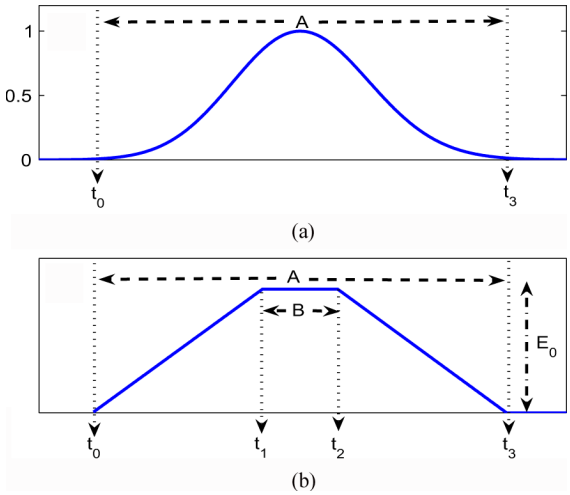

Fig. 1. Time distribution of (a) the single Brillouin pulse (SB), where A is the one percent time bandwidth of the pulse and (b) the single trapezoidal pulse, where E_0 is the maximum amplitude of the pulse and A and B are the bottom and top lengths of the single trapezoidal pulse, respectively.

$$f_{ST}(t) = \begin{cases} \left(\frac{1}{E_0}\right) t, & \text{for } t_0 < t < t_1 \\ E_0, & \text{for } t_1 < t < t_2 \\ -\left(\frac{1}{E_0}\right) t, & \text{for } t_2 < t < t_3 \end{cases} \tag{5}$$

where t_0 and t_3 are the points in time where the single Brillouin pulse is at one percent of its maximum amplitude and t_1 and t_2 are the beginning and end of the top of the single trapezoidal pulse. Fig. 1(a) and (b) shows the single Brillouin pulse along with the corresponding single trapezoidal pulse. The base $(t_3 - t_0)$ and the energy of the single trapezoidal pulses remains the same for different values of E_0. The top length of the single trapezoidal pulse (B) is calculated so that the energy of the pulse remains equal to the energy of the corresponding single Brillouin pulse for a specific value of (E_0). Hence, the trapezoidal pulses are linear approximations of the Brillouin pulse, under the constraint that their energy is the same. Fig. 2(a) and (b) shows the single and double Brillouin pulses along with the corresponding single and trapezoidal pulses of different amplitudes. Fig. 3 shows the frequency distribution of the double Brillouin pulse and double trapezoidal pulses. Note that the peaks of the spectral distribution of the double trapezoidal pulses are shifted to lower frequencies with respect to the peak for the double Brillouin pulse. This shift becomes smaller for larger trapezoidal pulse amplitudes.

The FDTD simulation of this problem is set up as follows. The entire computational domain is surrounded by a 10-cell perfectly matched layer (PML) [5]. In the simulations, the following space and time discretization parameters have been used: $\delta x = \delta z = \lambda_0/50$, $\delta t = s\delta x/\sqrt{2}c$ where $s = 0.7$ is the Courant stability number (λ_0 is the free space wavelength at the carrier frequency $f_c = 1$ GHz). The excitation is a point source which is located in the middle of the x-axis and $5\lambda_0$ away from the PML along the z-axis. The propagated field is sampled at consecutive points inside the medium on a straight line along the z-axis with the same x-coordinate as the source.

Fig. 4 depicts the peak value of the double Brillouin and double trapezoidal pulses at consequent sampling points inside the dispersive medium, normalized to the peak value of the field at the sampling point closest to the interface, for several values of E_0. Based on this figure,

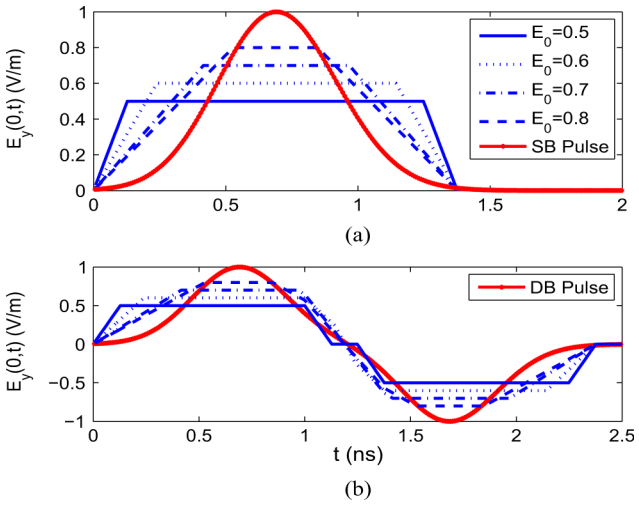

Fig. 2. Time distribution of (a) the single Brillouin pulse (SB) and single trapezoidal pulses with different amplitudes; (b) the double Brillouin pulse (DB) and double trapezoidal pulses with different amplitudes (E_0 defines the maximum amplitude of the pulse).

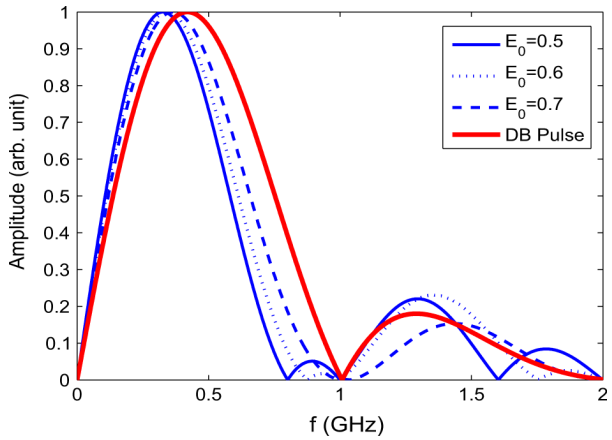

Fig. 3. Frequency distribution of the double Brillouin pulse (DB) and double trapezoidal pulses with different amplitudes.

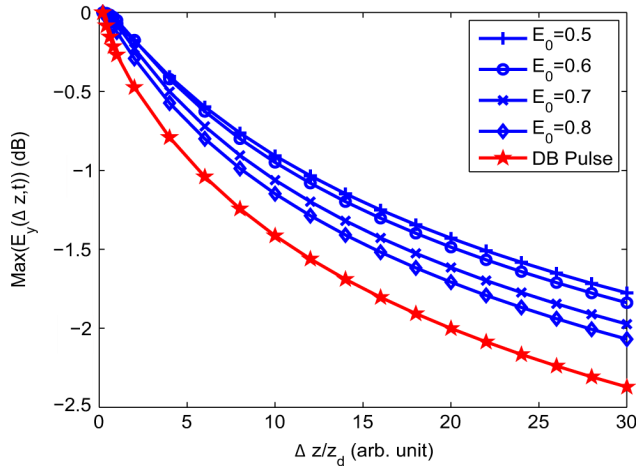

Fig. 4. Normalized peak amplitude of the double Brillouin and double trapezoidal pulses at consecutive observation points inside the dispersive medium (E_0 defines the maximum amplitude of the pulse and DB pulse is the double Brillouin pulse).

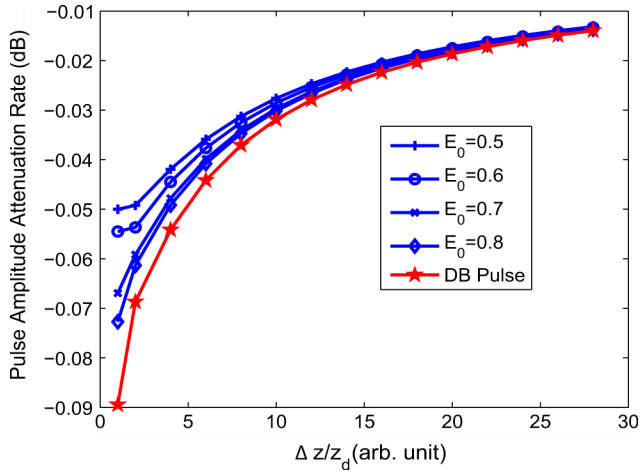

Fig. 5. Slope of the data presented in Fig. 4 (E_0 defines the maximum amplitude of the pulse and DB pulse is the double Brillouin pulse).

the attenuation rates of the double Brillouin and double trapezoidal pulses as a function of distance are calculated and shown in Fig. 5. Notably, while these rates differ for short distances (which is also evident from Fig. 4), they tend to become equal after a few absorption depths.

At short distances, the double Brillouin pulse attenuates slightly faster than the trapezoidal pulses, whose attenuation rates increase monotonically with E_0. This trend is due to the shift to lower frequencies shown for the spectra of the double trapezoidal pulses in Fig. 3, as lower frequency pulse harmonics have a larger penetration depth.

Furthermore, the study of the time-domain evolution of the trapezoidal pulses inside water shows that they eventually assume the shape of the double Brillouin pulse and, therefore, acquire its propagation characteristics. Fig. 6 shows the temporal evolution of a double trapezoidal pulse with $E_0 = 0.5$ at consecutive sampling points along its axis of propagation inside water. Evidently, the pulse assumes the shape of the double Brillouin pulse. Hence, while the early discrepancy between the attenuation rates of the pulses is due to their mutually shifted frequency spectra, the asymptotic agreement of these rates stems from the reshaping of the trapezoidal pulses into double Brillouin pulses. In conclusion, while having a double Brillouin source excitation is a sufficient condition for the generation of the Brillouin precursor inside water, it is not a necessary one.

III. Propagation of the Double Brillouin Pulse at Oblique Incidence

The interaction of the double Brillouin pulse with an air/water interface at oblique incidence is studied next, by means of the FDTD technique. Based on the previous section, our results are also applicable to trapezoidal pulses. Fig. 7 shows the 2-D FDTD computational domain (on the xz plane), which consists of two semi-infinite half-spaces: one of air and one of a Rocard–Powles–Debye medium. The excitation is a transverse electric (TE) wave ($E_y, H_x, H_z \neq 0$) which propagates in the z-direction. The source is in the free space region and it is excited along a row of cells parallel to the interface. The closed form of the excitation is

$$E_y(x, z_0) = f_{DB}\left(\frac{t - x\sin(\psi)}{c}\right)\exp\left[-\left(\frac{x - x_0}{10\lambda_0}\right)^2\right] \quad (6)$$

where $f_{DB}(t)$ is the function defined in (2), and ψ is the angle of incidence with respect to the normal to the interface. The parameter $x_0 = 4\lambda_0$ is a point on the x-axis where the maximum of the excitation

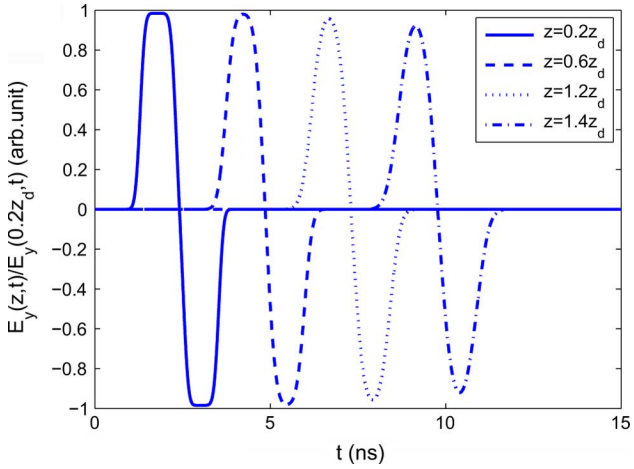

Fig. 6. Temporal evolution of the double trapezoidal pulse with $E_0 = 0.5$.

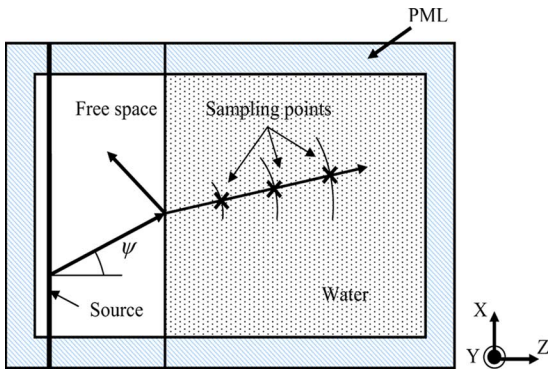

Fig. 7. Two-dimensional FDTD computational domain which models the infinite interface between the air and the Debye medium.

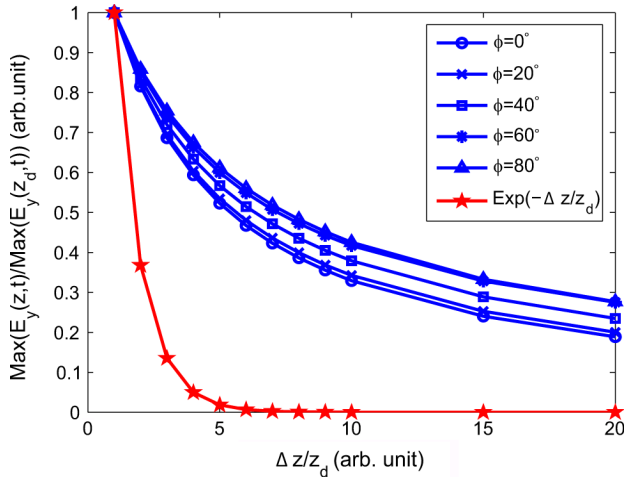

Fig. 8. Normalized peak amplitude of the double Brillouin pulse at consecutive observation points inside the dispersive medium for different incidence angles as compared to the exponential decay.

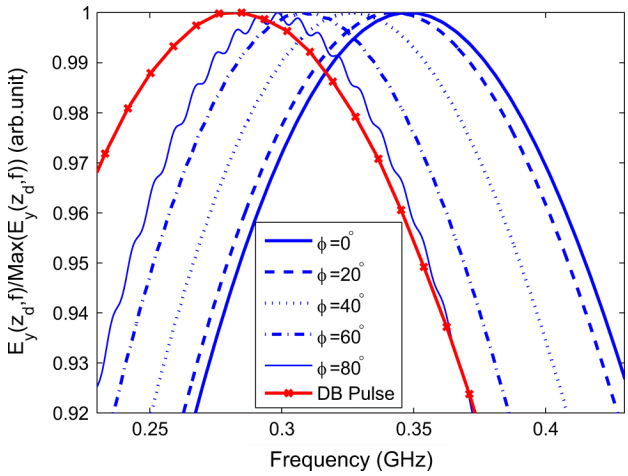

Fig. 9. Normalized Fourier transform of the double Brillouin propagated one absorption depth inside the dispersive medium as the incidence angle changes at the air/water interface and the Fourier transform of the double Brillouin pulse propagated in the infinite dispersive medium.

appears. The computational domain and its space and time discretization parameters are similar to the previous section. The source is along the x axis, 15 cells away from the left boundary of the computational domain ($z_0 = 15\delta z$). It illuminates the interface which is $10\lambda_0$ away from the source. The sampling points inside the dispersive medium are on circular paths, each of which with a radius that is an integer multiple of the absorption depth z_d.

Fig. 8 shows the normalized maximum amplitude of the double Brillouin pulse as the pulse propagates inside the medium for incident angles between 0 and 90 degrees (the value of the sampled field for each incidence angle is normalized with respect to the value of the field at the sampling point closest to the interface). It is clear that regardless of the angle of incidence, the double Brillouin pulse has a lower attenuation rate, compared to the normal exponential decay rate. Also, as the incidence angle increases the attenuation rate decreases. Hence, a performance degradation of the double Brillouin pulse, in terms of its attenuation rate, is observed closer to normal incidence. In the following, this degradation is explained first, and then compensated for.

This behavior can be explained by inspection of the transmission properties of the air-water interface as a function of the angle of incidence and frequency. The transmission coefficient for the interface, which is the ratio of the transmitted to the incident wave, for the TE polarization is given as [2]

$$T(\omega,\psi) = \frac{E_y^{\text{tran}}}{E_y^{\text{inc}}} = \frac{2n_1 n_2 \cos(\psi)}{\frac{\mu_1}{\mu_2} n_2^2 \cos(\psi) + n_1 \sqrt{n_2^2 - n_1^2 \sin(\psi)^2}} \tag{7}$$

where E_y^{inc} and E_y^{tran} are the incident and transmitted electric fields, respectively. For our case, $n_1 = 1$ and $n_2(\omega)$ is the dielectric constant of the dispersive medium which is given by (1). The absolute value of the transmission function decreases as the angle of incidence increases, and so does the amplitude of the transmitted pulse for the same excitation. Still, this does not explain the difference in attenuation for different angles observed in Fig. 8. This is accounted for by the fact that the transmission coefficient phase decreases almost linearly with respect to frequency, with the slope of this decrease becoming more negative as the angle of incidence increases. As a result, the interface effectively shifts the frequency content of the incident pulse to higher frequencies, with this shift being larger for smaller incidence angles of incidence.

To clarify this point, Fig. 9 depicts the power spectral density of the double Brillouin pulse one absorption depth inside the medium for different incidence angles, along with that of a double Brillouin pulse propagating in an infinite medium. The figure confirms the shift of the spectral support of the transmitted pulses compared to the original double Brillouin pulse, which increases with incidence angles closer

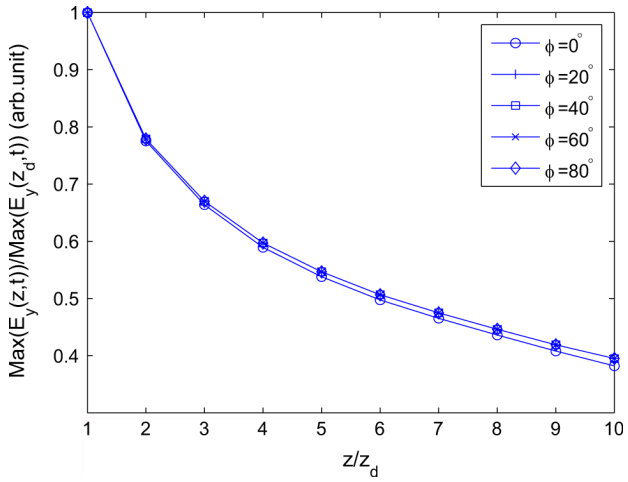

Fig. 10. Normalized peak amplitude of the modified double Brillouin pulse at consecutive observation points inside the dispersive medium for different incidence angles.

to normal. Hence, this perturbation of the spectral profile of the transmitted pulse from that of the double Brillouin pulse reduces its ability to excite the Brillouin precursor inside the medium, and consequently its ability to attain the Brillouin precursor's slow attenuation rate.

A simple remedy to the problem goes through the choice of an excitation shape that accounts for the effect of the interface. In particular, a modified excitation defined as

$$f_{\mathrm{DB}}^{\mathrm{modified}}(t) = F^{-1}\left\{S(\omega)\cdot\frac{1}{T(\omega,\psi)}\right\} \tag{8}$$

can be used, where, $F^{-1}\{.\}$ denotes an inverse Fourier transform and $S(\omega)$ is the Fourier transform of the double Brillouin pulse. Then, the transmitted pulse assumes the form of the double Brillouin pulse and recovers its attenuation properties. That is confirmed in Fig. 10, which repeats the experiment of Fig. 8 for the proposed excitation. Indeed, all transmitted pulses have identical attenuation properties in this case, independent of the angle of incidence.

IV. Summary and Conclusion

In this communication, two contributions to the problem of optimizing a pulse for low attenuation rate inside Debye media (and water, in particular) have been made. It has been shown that the critical factor for exciting a sub-exponentially attenuating Brillouin precursor inside water is not the shape, but rather the temporal support of the source. In particular, a class of trapezoidal pulses has been shown to be capable of generating the double Brillouin pulse of [4]. Furthermore, the problem of generating a double Brillouin pulse inside water from a source in air, illuminating water at oblique incidence, has been considered, since it corresponds to a practical scenario for underwater detection. It was pointed out that the effect of the interface undermines the excitation of the double Brillouin pulse, especially close to normal incidence, because it produces a spectral mismatch between the transmitted and the double Brillouin pulse. However, it was suggested that this effect can be readily compensated for, by appropriately modulating the source.

References

[1] L. Brillouin, *Wave Propagation and Group Velocity*. New York: Academic, 1960.

[2] J. D. Jackson, *Classical Electrodynamics*, 3rd ed. New York: Wiley, 1999.

[3] K. E. Oughstun and G. C. Sherman, *Electromagnetic Pulse Propagation in Causal Dielectrics*. Berlin, Germany: Springer-Verlag, 1994.

[4] K. E. Oughstun, "Dynamical evolution of the Brillouin precursor in Rocard–Powles–Debye model dielectrics," *IEEE Trans. Antennas Propag.*, vol. 53, no. 5, pp. 1582–1590, May 2005.

[5] A. Taflove and S. C. Hagness, *Computational Electromagnetics: The Finite-Difference Time-Domain Method*, 2nd ed. Norwood, MA: Artech House, 2000.

Simple Folded Monopole Slot Antenna for Penta-Band Clamshell Mobile Phone Application

Fang-Hsien Chu and Kin-Lu Wong

***Abstract*—An internal clamshell mobile phone antenna using a simple dual-band folded monopole slot for covering penta bands of WWAN operation is presented. The folded monopole slot has a length of about 60 mm only and is easily printed on the top portion (10×40 mm^2) of the main circuit board and suitable to be placed at the hinge of the clamshell mobile phone. By further placing the connecting strip between the two ground planes to be in the vicinity of the open end of the monopole slot, the two (main and upper) ground planes of the clamshell mobile phone can also be excited to be efficient radiators (dipole-like chassis or ground-plane modes excited through the strong electric field occurred at the slot's open end). By incorporating the resonant modes contributed from both the monopole slot and the two ground planes, two wide bands at about 900 and 1900 MHz are formed, which easily cover GSM850/900/1800/1900/UMTS operation. Owing to the additional resonant modes contributed by the two ground planes, the use of a simple folded monopole slot is sufficient to cover penta-band WWAN operation. This leads to compact size for the proposed clamshell mobile phone antenna. Details of the proposed antenna, including its SAR results, are presented.**

***Index Terms*—Antennas, handset antennas, mobile antennas, monopole slot antennas, multiband antennas.**

I. Introduction

The monopole slot or quarter-wavelength slot antenna can be operated at its 0.25λ resonant mode [1]–[16], different from the traditional slot antenna operated at the 0.5λ mode [17]. Owing to this attractive feature for the slot antenna to achieve a compact size, some promising monopole slot antennas suitable for application in the mobile devices such as the bar-type mobile phones [1]–[9], folder-type or clamshell mobile phones [10], and laptop computers [11], [12] have been demonstrated. In order not to complicate the circuit floor planning and signal line routing [4], the monopole slot antenna is not attractive to be placed in the center of the system ground plane of the mobile phone. However, in the case of the monopole slot antenna not placed at the center, the system ground plane is relatively difficult to be excited as an efficient radiator; in this case, it is required that at least

Manuscript received February 28, 2009; revised April 23, 2009. First published June 16, 2009; current version published November 04, 2009.

The authors are with the Department of Electrical Engineering, National Sun Yat-sen University, Kaohsiung 80424, Taiwan (e-mail: wongkl@ema.ee.nsysu.edu.tw; wongkl@mail.nsysu.edu.tw).

Color versions of one or more of the figures in this communication are available online at http://ieeexplore.ieee.org.

Digital Object Identifier 10.1109/TAP.2009.2025397